ASME Journal of Engineering for Sustainable Buildings and Cities
Online journal at:
https://asmedigitalcollection.asme.org/sustainablebuildings

Building Energy Savings and Power Output Augmentation of Roof Mounted Photovoltaic Using Co-Located Rooftop Reflectors

Habeeb Alasadi
Department of Mechanical and Aerospace Engineering,
University of Dayton,
300 College Park,
Dayton, OH 45469
e-mail: alasadih1@udayton.edu

Jun-Ki Choi
Department of Mechanical and Aerospace Engineering,
University of Dayton,
300 College Park,
Dayton, OH 45469
e-mail: jchoi1@udayton.edu

Rydge B. Mulford[1]
Department of Mechanical and Aerospace Engineering,
University of Dayton,
300 College Park,
Dayton, OH 45469
e-mail: rmulford1@udayton.edu

Photovoltaic (PV) panels installed on building rooftops yield a positive influence on the thermal performance of the building due to the shading of the PV panels, decreasing cooling loads while causing a smaller increase in heating loads. Additionally, the electrical power output of PV panels has been shown to be increased by including reflectors between PV rows, concentrating the solar flux onto the active portion of the panels. When implemented into the spaces between the rows of a roof-mounted PV array, reflectors might further improve the positive thermal effects of rooftop installed PV arrays. This work focuses on predicting rooftop heat flux and temperature for a building rooftop equipped with PV panels and reflectors. The saved energy load, additional energy load, PV power output, rooftop heat flux, and the utility factor (ratio of positive building energy impacts to negative building energy impacts) are reported parametrically for variations in the rooftop absorptivity and reflector area for three US locations. Utility factors of 375, 140, and 160 are found for Phoenix, AZ, Boise, ID, and Dayton, OH, respectively, for a reflector covering the full area between panels with a roof having a minimal absorptivity. A building in Phoenix, AZ exhibits a 15% increase in the utility factor of the PV-building system when reflectors are incorporated compared to a PV-building system without reflectors, while a building in Dayton, OH showed a 22% increase in utility factor when reflectors are included between the rows of a roof-mounted PV array. [DOI: 10.1115/1.4066795]

Keywords: PV-reflector shaded rooftops, reflector-augmented PV, reflector-PV-augmented roofs, roof temperature, heat flux through roofs, saved and additive energy, cooling and heating load of roofs, building heat transfer, integrated design, integrated systems, photovoltaics, renewable, sustainability

Introduction

Rooftop photovoltaic (PV) array installations provide electric power while utilizing acreage that has already been developed, minimizing environmental impact [1,2]. Further, the presence of PV arrays on rooftops positively influences building thermal behavior [3–12] by providing shading to the rooftop during hot summer months [13–16]. The value of PV array shading depends on the roof absorptivity, total shaded roof area, and local weather conditions.

A large number of publications have examined the power production of roof-mounted PV arrays [17–26], demonstrating arrays that generate between 16% and 50% of integrated building energy demand. Additional papers have modeled the influence of PV rooftop arrays on the heating and cooling loads due to the shading of rooftops caused by the PV panels. Models of building rooftops illustrate cooling savings between 5% and 35% when PV-covered rooftops are compared against uncovered rooftops [4,5,14,16,26–28]. The authors' recent publication focuses on quantifying the cooling savings during summer months as well as the additional energy required for heating as a result of PV shading [29] through modeling. It is shown that the utility factor, or ratio of produced energy and saved cooling energy to additional heating energy, of roof-mounted PV arrays can reach as high as 79 for hot locations in southerly latitudes. Experimental work [30] has shown that the cooling load of a shadowed roof declined 27.5% in a full 24 h and decreased about 37.4% between 08:00 a.m. and 05:00 p.m. The building cooling loads associated with removing heat transfer originating from the roof could be reduced by up to 23% for hot weather [31,32].

In summary, PV shading is beneficial for building thermal performance, and that the presence of reflectors improves PV performance. However, the literature has yet to consider the inclusion of reflectors into roof-mounted PV arrays and the resulting influence of these reflectors and PV panels on building thermal performance as well as PV efficiency and power production.

This work investigates the influence of roof-mounted, reflector-augmented PV arrays on rooftop cooling and calculates the heating loads and expected PV power output, accounting for the improved PV panel irradiation, increased panel temperature, and improved building shading. The utility factor, or ratio of annual electrical energy production and saved cooling energy to the additional heating energy, is used to quantify the benefits of PV and reflector shading on rooftops for three different locations in the US.

Methods

Energy Balance. Figures 1(*a*) and 1(*b*) present the 2D energy balances for both unshaded and PV-reflector-augmented rooftops. For an unshaded roof, diffuse and beam solar irradiation are absorbed by the roof and then conducted into the building, convected to the surrounding, and exchanged via radiation with the sky.

[1]Corresponding author.

Manuscript received May 21, 2024; final manuscript received October 2, 2024; published online October 18, 2024. Assoc. Editor: Dr. Andy Walker.

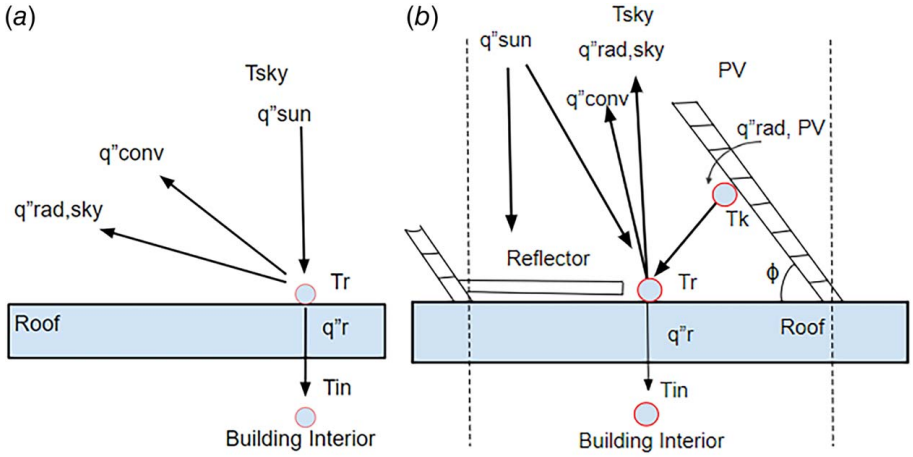

Fig. 1 (*a*) Energy balance on (*a*) unshaded roof and (*b*) shaded roof

For a PV-reflector augmented rooftop, diffuse and beam solar irradiation are absorbed by the PV array, rooftop, or the reflector. A portion of the irradiation incident on the reflector is reflected onto the PV panel or back into the surroundings. The absorbed energy conducts into the building, convects to the surrounding, and radiates into the sky or onto the building rooftop.

The energy balance for the unshaded baseline case is given as a heat flux balance in Eq. (1) and expanded as a function of temperature in Eq. (2). The energy input is absorbed solar energy heat flux $q''_{sun,abs}$ [33]. Energy leaves the surface due to conduction heat flux through the roof q''_{cond}, convection heat flux to the surrounding q''_{conv}, and the radiation heat exchange with the sky $q''_{rad,sky}$.

$$q''_{sun,abs} = q''_{cond} + q''_{conv} + q''_{rad,sky} \tag{1}$$

The heat conduction is a function of the unshaded and shaded roof temperatures (T_r, $T_{r,PV}$), building indoor temperature (T_{in} = 21 °C), the overall heat coefficient and convection coefficient of the roof (U = 0.19 W/m^2·K for Dayton, OH and Boise, ID and 0.23 W/m^2·K for Phoenix, AZ, $h_{in} = h_r = 3$ W/m^2·K) [34,35]. The absorptivity of the roof material is treated as a parameter in this work, varying between 0.2 and 0.8. The solar heat input is combination of the diffuse ($q''_{sun,d}$) and beam ($q''_{sun,b}$) solar components, where the beam component is scaled by the cosine of the angle between the roof normal and the sun's position (θ_b)

$$\alpha_r(q''_{sun,d} + q''_{sun,b}\cos\theta_b) = \frac{T_r - T_{in}}{\frac{1}{U} + \frac{1}{h_{in}}} + h_r(T_r - T_o) + \varepsilon_r\sigma(T_r^4 - T_{sky}^4) \tag{2}$$

An energy surface balance at the roof surface for the PV-reflector augmented roof case is presented in Fig. 1(*b*) and given in Eq. (3) and expanded in Eq. (4). The reflector and exposed roof are assumed to be in sufficient thermal contact such that they are isothermal at the same temperature ($T_{r,PV}$). The energy entering the system is the summation of absorbed solar heating to the roof and the reflector ($q''_{sun,abs}$) and the radiative heat flux from the back of the PV onto the exposed roof and the reflector ($q''_{rad,PV}$). The energy leaving the system is the combination of the heat conduction into the building (q''_{cond}), the heat radiation to the sky from both the exposed roof material and the reflector material ($q''_{rad,sky}$), and the heat convection to the surroundings (q''_{conv}). In Eq. (4), the subscript r indicates the uncovered roof section between PV panels and the subscript f indicates the reflector panel covering a portion of the roof. The PV and roof are assumed to be opaque, gray, and diffuse, and the gray reflector reflects the beam component of solar irradiation with a specularity of 50% and the diffuse component of solar irradiation in a completely diffuse fashion.

$$q''_{cond} + q''_{conv} + q''_{rad,sky} = q''_{rad,PV} + q''_{sun,abs} \tag{3}$$

$$\begin{aligned}&\frac{T_{r,PV} - T_{in}}{\frac{1}{U} + \frac{1}{h_{in}}} + h_r(T_{r,PV} - T_o) + \varepsilon_r\sigma F_{r,sky}(T_{r,PV}^4 - T_{sky}^4)\\ &+ \varepsilon_f\sigma F_{f,sky}(T_{r,PV}^4 - T_{sky}^4) = \alpha_r\varepsilon_{PV}\sigma F_{PV,r}(T_{PV}^4 - T_{r,PV}^4)\\ &+ \alpha_f\varepsilon_{PV}\sigma F_{PV,f}(T_{PV}^4 - T_{r,PV}^4) + q''_{sun,abs}\end{aligned} \tag{4}$$

The absorbed heat flux from the sun for the reflector and exposed roof surface ($q''_{sun,abs}$) is given by Eq. (5) and consists of the beam and diffuse components absorbed by the roof and reflector. The diffuse solar component is assumed to be incident on the opening between the two solar panels, labeled with the subscript *sky*, and the view factor scales the diffuse component to determine the fraction that is incident on the exposed roof ($F_{sky,r}$) and the reflector ($F_{sky,f}$). Due to shading from the PV panels, the reflector and exposed roof area will receive a varying percentage of total beam irradiation incident on the full roof area. The shading fraction of the exposed roof (λ_r) and reflector (λ_f) is the ratio of area illuminated by beam irradiation to the total area of the component [36].

$$\begin{aligned}&q''_{sun,abs} = q''_{sun,d,r} + q''_{sun,d,f} + q''_{sun,b,r} + q''_{sun,b,f} =\\ &(\alpha_r F_{sky,r} + \alpha_f F_{sky,f})q''_{sun,d} + (\alpha_r\lambda_r + \alpha_f\lambda_f)q''_{sun,b}\cos\theta_b\end{aligned} \tag{5}$$

The sky temperature was calculated using the ambient temperature [37,38] and the PV back surface temperature was calculated using the ambient temperature and solar heat flux [37,38]. The PV temperature is obtained from the ambient temperature and the PV heat flux while the PV power output was obtained from the PV specification and PV heat flux [39–41].

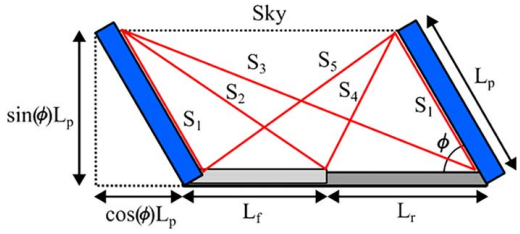

Fig. 2 Dimensions used to calculate the view factors between the reflector and sky and the exposed roof and the sky. The PV panels are depicted as angled boxes with a tilt angle of *f* while the reflector and roof (horiziontal boxes) are shown between the two panels. The dimensions S_1, S_2, S_3, S_4, and S_5 are used to calculate the view factors as given in Eqs. (10)–(16).

View Factors. Two view factors are necessary for the evaluation of Eq. (5), specifically the view factor from the reflector to the surroundings and the view factor from the exposed roof surface to the surroundings. Assuming again a two-dimensional model, the view factors may be calculated using Hottel's crossed strings method using the lengths as depicted in Fig. 2 [36]. The view factors are calculated using Eqs. (10) and (11), with the values for S_1, S_2, S_3, S_4, and S_5 given in Eqs. (12)–(16).

$$F_{f-sky} = \frac{(S_2 + S_5) + (S_1 + S_3)}{2L_f} \tag{6}$$

$$F_{r-sky} = \frac{(S_4 + S_3) + (S_1 + S_2)}{2L_r} \tag{7}$$

$$S_1 = L_p \tag{8}$$

$$S_2 = [(L_f + \cos(\phi)L_p)^2 + (\sin(\phi)L_p)^2]^{1/2} \tag{9}$$

$$S_3 = [(\sin(\phi)L_p)^2 + (L_r - \cos(\phi)L_p)^2]^{1/2} \tag{10}$$

$$S_4 = [(L_f + L_r + \cos(\phi)L_p)^2 + (\sin(\phi)L_p)^2]^{1/2} \tag{11}$$

$$S_5 = [(L_f + L_r - \cos(\phi)L_p)^2 + (\sin(\phi)L_p)^2]^{1/2} \tag{12}$$

Result Metrics. The annual saved energy load (SEL), shown in Eq. (6), is calculated by subtracting the annual heat flux through the unshaded roof from the flux through the roof shaded by both PV and the reflector, then dividing by the building's climate control system's COP. SEL measures the energy saved from shading by the reflector and PV panels, adjusted for cooling system efficiency. Conversely, the additional energy load (AEL), defined in Eq. (7), is found by subtracting the heat flux for shaded and unshaded models and dividing it by the heating system's efficiency. AEL indicates the extra energy required for heating due to reduced solar heating from shading. SEL applies when heat flux moves from the roof to the interior, while AEL applies when it moves from the interior to the exterior. Both SEL and AEL are influenced by the roof's R-value: lower thermal resistance increases SEL and AEL, enhancing the PV panels' impact on energy performance, while higher resistance reduces this effect.

$$\text{SEL} = \frac{\sum q''_r - \sum q''_{r,PV}}{\text{COP}}, \quad q''_r > q''_{r,PV+f} \tag{13}$$

$$\text{AEL} = \frac{\sum q''_{r,PV} - \sum q''_r}{\eta_{heat}}, \quad q''_r < q''_{r,PV+f} \tag{14}$$

The utility factor for the PV system, defined in Eq. (8), is the sum of SEL and PV power output divided by SEL. It measures the PV panels' impact on building energy balance. The numerator combines energy conserved by shading and electrical energy from the PV system, while the denominator includes additional energy needed to maintain thermal set points due to shading. A utility factor of one means PV panels produce and consume an equivalent amount of energy as the building's baseload. Values above one indicate a greater positive impact of the PV panels.

$$\Psi = \frac{\text{SEL} + P_{PV}}{\text{AEL}} \tag{15}$$

Equations (1)–(5) represent the full thermal model used to investigate the results in this study, and Eqs. (6)–(8) give the metrics used to discuss the results. This work uses the TMY3 hourly weather condition data for expected solar heat fluxes for each hour of the year over a typical meteorological year. The result metrics are calculated for both shaded and unshaded rooftops for three cities in the US.

Locations and Photovoltaic Model Specification. This work investigates three different locations in the US: Dayton, OH, Boise, ID, and Phoenix, AZ. The three cities are located in different climate zones. The ambient temperature, beam irradiation, and cloud percentage of each location are presented in Table 1. The data are the average of three winter months (December, January, and February) and the average of three summer months (June, July, and August). Table 2 presents the specifications of PV module, roof, and ambient conditions for the three cities, assuming a PV panel that is 1 m in height.

Parametric Study. The result metrics vary as a function of rooftop parameters, including the optical properties of the rooftop as well as the percentage of the rooftop area covered by reflectors relative to the total rooftop area. In this study, the SEL, AEL, and utility factor are calculated for three cities as a function of rooftop absorptivity, expressed from 0.2 to 0.8 in increments of 0.2, and the size of the reflector, defined as the area of the reflector on the rooftop divided by the total area of the rooftop, expressed from 0 to 0.5 in increments of 0.1.

Results

Rooftop Temperature. Figure 3 presents comparison of the daily average ambient temperature and unshaded and shaded roof temperatures in Dayton, OH and Phoenix, AZ in July and December. Figures 3(*a*) and 3(*b*) illustrate that, during summer months, the daily average temperature of the unshaded roof is consistently higher than the shaded and ambient temperatures in July, while the shaded roof temperature is consistently higher than ambient temperature. The only exception is cloudy days (day 8 in Fig. 3(*a*)), where the shading provided by the PV panels and reflectors provides no advantage.

During the winter, however, the Dayton, OH unshaded and shaded roof temperatures are roughly equivalent, with the shaded roof temperature generally showing a slight increase in temperature (by 1–2 °C) relative to the unshaded rooftop. The PV panels act as a buffer against the cold night sky, causing the radiative losses from the shaded roof to be less than the unshaded roof, increasing slightly the average rooftop temperature in winter months for the shaded roof. Likewise, Fig. 3(*d*) depicts the temperature behavior of shaded and unshaded roofs in Phoenix, AZ during December. Unlike Dayton, OH, Phoenix, AZ continues to experience relatively little cloud cover in the winter months. In this case, the unshaded

Table 1 Winter and summer average temperature, average daily beam irradiation, and average cloud percentage [40]

	Winter			Summer		
	Temperature (°C)	Beam irradiation (Wh/m^2)	Cloud (%)	Temperature (°C)	Beam irradiation (Wh/m^2)	Cloud (%)
Dayton, OH	0.68	70.47	77.95	22.84	230.42	61.29
Boise, ID	0.91	76.68	73.01	21.87	302.66	27.58
Phoenix, AZ	13.39	145.18	36.93	34.46	320.00	33.22

Table 2 Roof, PV, reflector, and air conditioning specifications

	Dayton, OH	Phoenix, AZ	Boise, ID
Roof area (m^2)	1800	1800	1800
PV tilt angle (deg)	33 deg	28 deg	36 deg
$L_f + L_r$ (panel spacing) (m)	2.87	2.17	3
PV area (m^2)	626	828	599
COP [42]	3.6	3.6	3.6
Heating efficiency [43]	0.96	0.96	0.96

roof temperature is higher than both the shaded roof and the ambient temperature in most of the December hours.

Roof Heat Flux. For all three locations, the heat flux into the unshaded rooftop is consistently higher than the heat flux into the PV shaded rooftop, with the shaded heat flux exhibiting reductions of up to 45% compared to the unshaded heat flux depending on location and time of year. Reductions in heat flux are most prominent during sunny, summer days and are the largest in Phoenix, AZ, with the smallest reductions in heat flux in Dayton, OH.

Additional Energy Load and Saved Energy Load. Figure 4 shows the SEL and AEL for the PV-reflector system, based on roof absorptivity and reflector coverage ratio. For brevity, only results for Dayton, OH are depicted in Fig. 4. The trends in the Dayton, OH results are generally applicable across all locations tested. Increasing reflector area or roof absorptivity generally raises both SEL and AEL. Absorptivity affects SEL more significantly than AEL, with SEL increasing almost an order of magnitude across locations, while AEL roughly doubles as absorptivity rises from 0.2 to 0.8.

The reflector area ratio has a direct impact: increasing the area ratio for roofs with absorptivity above 0.3 raises SEL and AEL, while for roofs with absorptivity below 0.3, it reduces both. For high absorptivity values, SEL increases linearly and AEL increases parabolically.

Utility Factor and Reflector Effectiveness. Utility factor decreases with higher roof absorptivity and increases with a larger reflector-to-roof ratio. Table 3 shows that maximum utility factors are 135, 160, and 360 for Dayton, OH, Boise, ID, and Phoenix, AZ, respectively. Maximum reflector effectiveness values are 0.24, 0.19, and 0.15, with minima of −0.30, −0.13, and −0.18. The negative reflector effectiveness values generally correlate to a large area ratio and roof absorptivity, whereas the maximum reflector effectiveness values are found at the lowest rooftop absorptivity values and the highest reflector area ratio.

Discussion

Saved Energy Load and Additional Energy Load. Figure 4 shows that SEL depends on roof absorptivity and reflector coverage. The highest SEL is seen with the highest roof absorptivity and maximum reflector coverage. High absorptivity roofs absorb more solar radiation, leading to greater energy savings compared

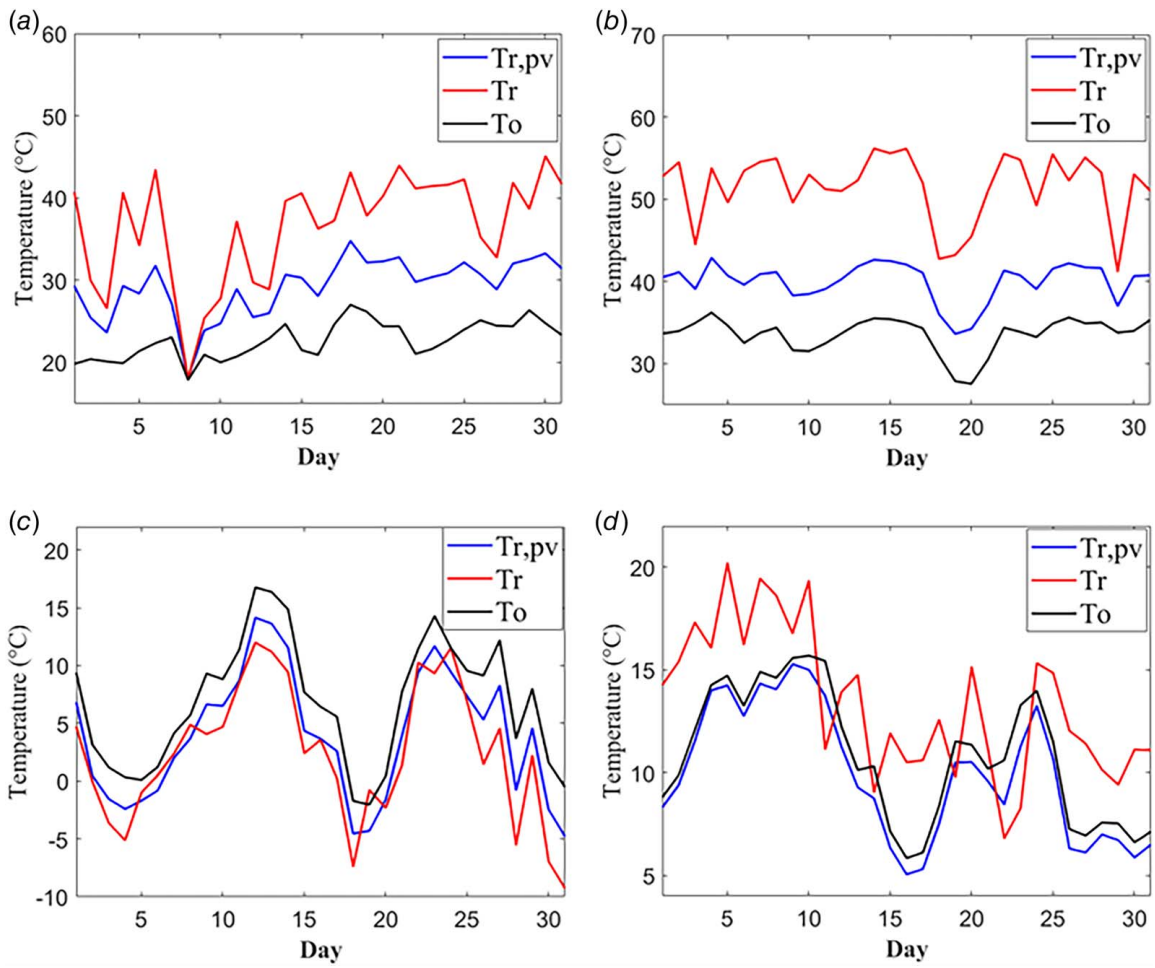

Fig. 3 Results for Dayton, OH and Phoenix, AZ, including daily average ambient temperature and roof temperature without (T_r) and with ($T_{r,PV}$) PV panel shading: (*a*), (*b*) during July, and (*c*), (*d*) during December; (*a*) and (*c*) are for Dayton, OH, and (*b*) and (*d*) are for Phoenix, AZ

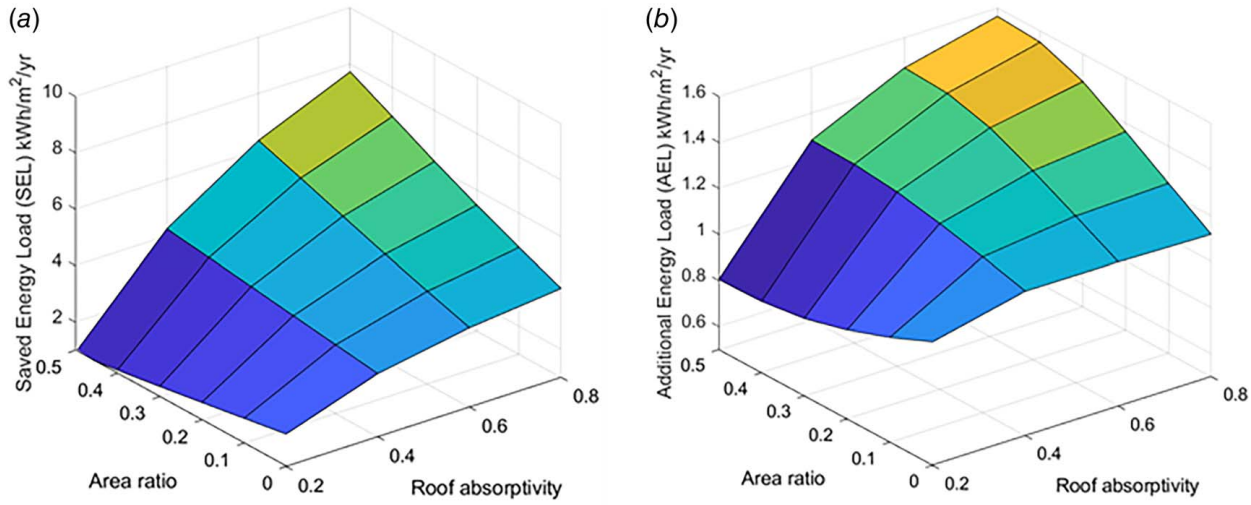

Fig. 4 (*a*) SEL and (*b*) AEL for Dayton, OH

Table 3 Utility factor and reflector effectiveness for the three cities

	Dayton, OH	Boise, ID	Phoenix, AZ
Maximum utility factor	135	160	360
Maximum reflector effectiveness	0.24	0.19	0.15
Minimum reflector effectiveness	−0.30	−0.13	−0.18

to low absorptivity roofs. At a roof absorptivity of 0.2, which is lower than the reflector's 0.25, reflectors have minimal impact on roof thermal performance. However, the reflected solar irradiation enhances PV performance by about 0.5 kWh/m^2/year, varying by location. For roofs with absorptivity below 0.2, the roof itself reflects more efficiently than the reflector material, encouraging the reflector area to go to zero. With no reflector coverage, the PV panels alone influence building thermal performance. Increased roof absorptivity improves the shading effect of PV panels, reducing solar heat absorption into the building.

Utility Factor. The utility factor rises as roof absorptivity decreases and as reflector coverage increases (for low absorptivity). With low absorptivity and high coverage, the roof area shaded by PV panels doesn't absorb direct sunlight, reducing winter heating. However, the uncovered roof can still lose heat by radiation to the cold night sky. Lower roof absorptivity decreases thermal losses in winter. Regionally, Phoenix, AZ has a higher utility factor (375) compared to Dayton, OH (140) and Boise, ID (160). This is due to increased solar output from reflected irradiation and reduced winter radiative cooling. These results suggest roof reflectors enhance the economic benefits of PV arrays, particularly in sunny areas like Phoenix, AZ.

Reflector Effectiveness. Reflector effectiveness measures the energy impact of reflectors on building energy system performance. Positive values indicate a benefit, while negative values show a decrease in performance. High roof absorptivity leads to negative effectiveness, while low absorptivity yields positive values. As roof coverage approaches 0%, the effect of roof absorptivity diminishes. Reflectors have a greater impact in colder, cloudier climates (e.g., Dayton, OH) compared to sunnier, drier ones (e.g., Phoenix, AZ), with maximum effectiveness values of 0.22 and 0.15, respectively. In summer, high-absorptivity roofs absorb sunlight, increasing cooling loads, while low-absorptivity reflectors reflect sunlight to PV panels, enhancing electricity production. In winter, reflectors reduce radiative cooling but can overheat panels in hot climates like Phoenix, AZ, reducing efficiency.

Future considerations include the potential voiding of PV warranties with reflectors and the risk of material degradation. Bifacial PV modules, which capture energy on both sides of the PV panel, could offer additional power and should be evaluated for their thermal and electrical performance benefits.

Conclusion

The addition of a PV-reflector system on building rooftops reduces solar irradiation falling on the roof, resulting in cooling energy savings in summer months but requiring additional heating energy in winter months. The presence of a reflector on the rooftop surface was explored in this work to determine its overall impact on the thermal and electrical performance of the PV-building energy system. Results show that a PV-reflector system on the rooftop reduces roof temperatures during summer months while maintaining the rooftop temperature near the ambient temperature during winter months.

Parametrically, it is shown that the utility factor for all three locations increases as the roof absorptivity decreases and increases as the roof area covered by the reflector increases owing to the reduction of radiative cooling from the roof surface during winter months. Sunny, dry locations exhibit much higher utility factors, with a maximum value of 375 calculated for Phoenix, AZ as compared to 140 and 160 for Dayton, OH and Boise, ID, respectively. The utility of the reflector individually is likewise calculated with the reflector effectiveness. For cases where the roof is at least 50% covered with reflector and the roof absorptivity is high (0.8), the reflector increases system thermal performance by as much as 22%. However, for low roof absorptivities (0.2), the reflector has a detrimental impact on the roof performance. Likewise, increasing the coverage area of the reflector increases the utility of the reflector and vice versa.

Acknowledgment

The authors would like to acknowledge the contributions of Dr. Robert Gilbert for the initial discussion regarding this work.

Funding Data

- The US Department of Energy for supporting this work through its funding of the Industrial Assessment Center program (DE-EE0007710).

Conflict of Interest

There are no conflicts of interest.

Data Availability Statement

The datasets generated and supporting the findings of this article are obtainable from the corresponding author upon reasonable request.

Nomenclature

h = convection coefficient (W/(m^2·K))
A = area (m^2)
F = view factor
I = irradiation (w/m^2)
L = length (m)
P = power (W)
T = temperature (K)
U = overall heating coefficient (W/(m^2·K))
q'' = heat flux (W/m^2)
AEL = additional energy load (W/m^2)
COP = coefficient of performance
SEL = saved energy load (W/m^2)
α = absorptivity
ε = emissivity
η = efficiency
θ = sun elevation (deg)
λ = shading fraction
σ = Stefan–Boltzmann constant (W/(m^2·K^4))
ϕ = PV tilt angle (deg)
Ψ = utility factor

Subscripts

b = beam irradiation
d = diffuse
f = reflector
k = back of PV panel
abs = absorbed
con = convection
$heat$ = building heating system
in = inside
PVo = PV panel outside
rPV = roof PV panel
$radr$ = radiation roof
rad = radiation

References

[1] Hong, T., Lee, M., Koo, C., Jeong, K., and Kim, J., 2017, "Development of a Method for Estimating the Rooftop Solar Photovoltaic (PV) Potential by Analyzing the Available Rooftop Area Using Hillshade Analysis," Appl. Energy, **194**, pp. 320–332.
[2] Cao, X., Dai, X., and Liu, J., 2016, "Building Energy-Consumption Status Worldwide and the State-of-the-Art Technologies for Zero-Energy Buildings During the Past Decade," Energy Build., **128**, pp. 198–213.
[3] Maghrabie, H. M., Elsaid, K., Sayed, E. T., Abdelkareem, M. A., Wilberforce, T., and Olabi, A. G., 2021, "Building-Integrated Photovoltaic/Thermal (BIPVT) Systems: Applications and Challenges," Sustain. Energy Technol. Assess., **45**, p. 101151.
[4] Singh, D., and Chaudhary, R., 2021, "Impact of Roof Attached Photovoltaic Modules on Building Material Performance," Mater. Today: Proc., **46**, pp. 445–450.
[5] Maqbool, M. U., Butt, A. D., Bhatti, A. R., Sheikh, Y. A., and Asif, M. W., 2021, "Impact of Rooftop PV Shading on Net Electrical Energy Demand of Buildings in Pakistan," Sci. Proc. Ser., **3**(1), pp. 45–49.
[6] Alrashidi, H., Ghosh, A., Issa, W., Sellami, N., Mallick, T. K., and Sundaram, S., 2020, "Thermal Performance of Semitransparent CdTe BIPV Window at Temperate Climate," Sol. Energy, **195**, pp. 536–543.
[7] Alrashidi, H., Issa, W., Sellami, N., Sundaram, S., and Mallick, T., 2022, "Thermal Performance Evaluation and Energy Saving Potential of Semi-Transparent CdTe in Façade BIPV," Sol. Energy, **232**, pp. 84–91.
[8] Yu, G., Yang, H., Luo, D., Cheng, X., and Ansah, M. K., 2021, "A Review on Developments and Researches of Building Integrated Photovoltaic (BIPV) Windows and Shading Blinds," Renewable Sustainable Energy Rev., **149**, p. 111288.
[9] Krarti, M., 2021, "Performance of PV Integrated Dynamic Overhangs Applied to US Homes," Energy, **230**, p. 120843.
[10] Cavadini, G. B., and Cook, L. M., 2021, "Green and Cool Roof Choices Integrated Into Rooftop Solar Energy Modelling," Appl. Energy, **296**(May), p. 117082.
[11] Sheikh, Y. A., Maqbool, M. U., Butt, A. D., Bhatti, A. R., Awan, A. B., Paracha, K. N., and Khan, M. M., 2021, "Impact of Rooftop Photovoltaic on Energy Demand of a Building in a Hot Semi-Arid Climate," J. Renew. Sustain. Energy, **13**(6), p. 117082.
[12] Elghamry, R., Hassan, H., and Hawwash, A. A., 2020, "A Parametric Study on the Impact of Integrating Solar Cell Panel at Building Envelope on Its Power, Energy Consumption, Comfort Conditions, and CO2 Emissions," J. Clean. Prod., **249**, p. 119374.
[13] Park, J. H., Yun, B. Y., Chang, S. J., Wi, S., Jeon, J., and Kim, S., 2020, "Impact of a Passive Retrofit Shading System on Educational Building to Improve Thermal Comfort and Energy Consumption," Energy Build., **216**, p. 109930.
[14] D'Agostino, D., Parker, D., Melià, P., and Dotelli, G., 2022, "Optimizing Photovoltaic Electric Generation and Roof Insulation in Existing Residential Buildings," Energy Build., **255**, p. 111652.
[15] Abuseif, M., and Gou, Z., 2018, "A Review of Roofing Methods: Construction Features, Heat Reduction, Payback Period and Climatic Responsiveness," Energies (Basel), **11**(11), p. 3196.
[16] Kapsalis, V. C., Vardoulakis, E., and Karamanis, D., 2014, "Simulation of the Cooling Effect of the Roof-Added Photovoltaic Panels," Adv. Build. Energy Res., **8**(1), pp. 41–54.
[17] Gassar, A. A. A., and Cha, S. H., 2022, "Feasibility Assessment of Adopting Distributed Solar Photovoltaics and Phase Change Materials in Multifamily Residential Buildings," Sustain. Prod. Consum., **29**, pp. 507–528.
[18] Monna, S., Abdallah, R., Juaidi, A., Albatayneh, A., Zapata-Sierra, A. J., and Manzano-Agugliaro, F., 2022, "Potential Electricity Production by Installing Photovoltaic Systems on the Rooftops of Residential Buildings in Jordan: An Approach to Climate Change Mitigation," Energies (Basel), **15**(2), p. 496.
[19] Mehadi, A. A., Chowdhury, M. A., Nishat, M. M., Faisal, F., and Islam, M. M., 2021, "A Software-Based Approach in Designing a Rooftop Bifacial PV System for the North Hall of Residence, IUT," Clean Energy, **5**(3), pp. 403–422.
[20] Odeh, S., 2018, "Thermal Performance of Dwellings With Rooftop PV Panels and PV/Thermal Collectors," Energies (Basel), **11**(7), p. 1879.
[21] Dehwah, A. H. A., and Asif, M., 2019, "Assessment of Net Energy Contribution to Buildings by Rooftop Photovoltaic Systems in Hot-Humid Climates," Renewable Energy, **131**, pp. 1288–1299.
[22] Ogbeba, J. E., and Hoskara, E., 2019, "The Evaluation of Single-Family Detached Housing Units in Terms of Integrated Photovoltaic Shading Devices: The Case of Northern Cyprus," Sustainability (Switzerland), **11**(3), p. 593.
[23] Alghamdi, A. S., 2021, "Performance Enhancement of Roof-Mounted Photovoltaic System: Artificial Neural Network Optimization of Ground Coverage Ratio," Energies (Basel), **14**(6), p. 1537.
[24] Kaji Esfahani, S., Tenorio, R., Karrech, A., Defendi, K., and Jerez, F., 2021, "Analysing the Role of Roof Mounted BIPV System Optimization on Decreasing the Effect of Duck Curve in Perth, Western Australia: An Experimental Case Study," Sustain. Energy Technol. Assess., **47**, p. 101328.
[25] Jahanfar, A., Sleep, B., and Drake, J., 2018, "Energy and Carbon-Emission Analysis of Integrated Green-Roof Photovoltaic Systems: Probabilistic Approach," J. Infrastruct. Syst., **24**(1), p. 04017044.
[26] Rahmani, F., Robinson, M. A., and Barzegaran, M. R., 2021, "Cool Roof Coating Impact on Roof-Mounted Photovoltaic Solar Modules at Texas Green Power Microgrid," Int. J. Electr. Power Energy Syst., **130**, p. 106932.
[27] Ibrahim, M., Shehata, A., Elharidi, A., and Hanafy, A., 2021, "Effect of PV Shadow on Cooling Load and Energy Consumption of Zone Toward Achieving NZEB," IOP Conf. Ser. Earth Environ. Sci., **801**(1), p. 012027.
[28] Peng, C., and Yang, J., 2016, "The Effect of Photovoltaic Panels on the Rooftop Temperature in the EnergyPlus Simulation Environment," Int. J. Photoenergy, **2016**, pp. 1–12.
[29] Alasadi, H., Choi, J. K., and Mulford, R. B., 2022, "Influence of Photovoltaic Shading on Rooftop Heat Transfer, Building Energy Loads, and Photovoltaic Power Output," ASME J. Sol. Energy Eng., **144**(6), p. 061011.
[30] Liu, S., Yan, Y., Zhang, Z., and Bai, J., 2019, "Effect of Distributed Photovoltaic Power Station on Cooling Load Induced by Roof for Sunny Day in Summer," Ther. Sci. Eng. Prog., **10**, pp. 36–41.
[31] Zubair, M., Awan, A. B., and Praveen, R. P., 2018, "Analysis of Photovoltaic Arrays Efficiency for Reduction of Building Cooling Load in Hot Climates," Build. Serv. Eng. Res. Technol., **39**(6), pp. 733–748.
[32] Peres, A. C., Calili, R., and Louzada, D., 2020, "Impacts of Photovoltaic Shading Devices on Energy Generation and Cooling Demand," Conference Record of the IEEE Photovoltaic Specialists Conference, Virtual, June, pp. 1186–1191.
[33] Gentle, A. R., Aguilar, J. L. C., and Smith, G. B., 2011, "Optimized Cool Roofs: Integrating Albedo and Thermal Emittance With R-Value," Sol. Energy Mater. Sol. Cells, **95**(12), pp. 3207–3215.
[34] Jarnagin, R. F., McBride, M. F., and Colliver, D. G., 2006, "Advanced Energy Design Guide for Small Retail Buildings," ASHRAE J., **48**(9), p. 117.
[35] Saidi, M., and Abardeh, R. H., 2010, "Air Pressure Dependence of Natural-Convection Heat Transfer," WCE 2010—World Congress on Engineering 2010, London, UK, June 30–July 2, Vol. 2, pp. 1444–1447.
[36] Modest, M. F., 2013, *Radiative Heat Transfer*, Academic Press, New York, NY.
[37] Davis, M. W., Fanney, A. H., and Dougherty, B. P., 2003, "Measured Versus Predicted Performance of Building Integrated Photovoltaics," ASME J. Sol. Energy Eng., **125**(1), pp. 21–27.

[38] Wang, D., Qi, T., Liu, Y., Wang, Y., Fan, J., Wang, Y., and Du, H., 2020, "A Method for Evaluating Both Shading and Power Generation Effects of Rooftop Solar PV Panels for Different Climate Zones of China," Sol. Energy, **205**(13), pp. 432–445.
[39] Duffie, J. A., and Beckman, W. A., 1991, *Solar Engineering of Thermal Processes*, 2nd ed., Wiley, New York, NY.
[40] Alasadi, H., Choi, J. K., and Mulford, R. B., 2022, "Influence of Photovoltaic Shading on Rooftop Heat Transfer, Building Energy Loads, and Photovoltaic Power Output," ASME J. Sol. Energy Eng., **144**(6), p. 060801.
[41] Alasadi, H., Mulford, R., and Gilbert, R., 2020, "Reflector-Augmented Photovoltaic Power Output Incorporating Temperature-Dependent Photovoltaic Efficiency," ASME International Mechanical Engineering Congress and Exposition Proceedings (IMECE), Vol. 8, pp. 1–6.
[42] Astrain, D., Merino, A., Catalán, L., Aranguren, P., Araiz, M., Sánchez, D., Cabello, R., and Llopis, R., 2019, "Improvements in the Cooling Capacity and the COP of a Transcritical CO2 Refrigeration Plant Operating With a Thermoelectric Subcooling System," Appl. Therm. Eng., **155**, pp. 110–122.
[43] U.S. Department of Energy, "Incorporate Minimum Efficiency Requirements for Heating and Cooling Products Into Federal Acquisition Documents," https://www.energy.gov/eere/femp/incorporate-minimum-efficiency-requirements-heating-and-cooling-products-federal, Accessed May 28, 2021.